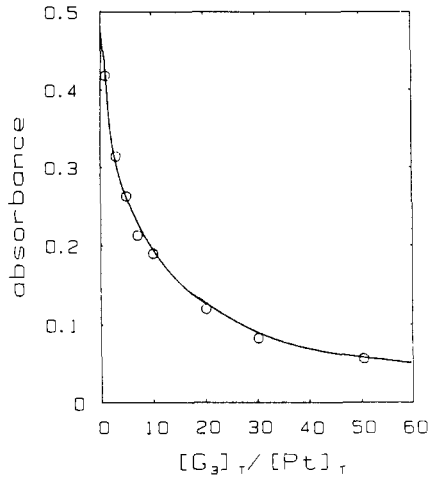

Figure 10. Absorbance dependence on excess $[G_3]$ to give $Pt(H_{-1}G_3)_2^{2-}$ (VI) ($[Pt]_T = 9.90 \times 10^{-4}$ M, $[Cl^-]_T = 3.96 \times 10^{-3}$, [phosphate]$_T$ = 0.10 M, -log $[H^+]$ = 7.0, μ = 1.0 M ($NaClO_4$), 25.0 °C, 260 nm, 1-mm cell path).

$\times 10^3$ M^{-1}. This constant was measured in the presence of 0.1 M phosphate buffer at pH 7.0 with 9.9×10^{-4} M $[Pt]_T$ (Figure 10). The equilibrium constant K_4 is smaller by a factor of 20 than the corresponding constant determined for Pd(II) (1.6×10^5 M^{-1})[37] but is much larger than the value for Cu(II) (1.74×10^2 M^{-1}).[38]

Conclusions

Deprotonated-N(peptide) complexation to Pt(II) occurs even in acidic solutions with high Cl^- concentrations. After 1 week, the reaction of $PtCl_4^{2-}$ with triglycine gives $Pt(H_{-2}G_3)Cl^{2-}$ as the major species (>60%) in 0.65 M Cl^- at pH 3.85. Since the platinum(II) chloride complexes are quite strong (i.e. $[PtCl_4^{2-}]/([PtCl^+][Cl^-]^3) = 10^{9.0}$ M^{-3}), this indicates that Pt-N^-(peptide) bond formation in the absence of Cl^- should occur below pH 1. However, the initial coordination reaction is extremely slow in acid. Our results show that platinum forms much stronger M(II)-N(peptide) bonds than copper,[1] nickel,[3] or palladium.[5] On the other hand, when a third N^-(peptide) group coordinates, as in $M^{II}(H_{-3}G_4)^{2-}$, relatively high pH is needed to give the corresponding platinum complex. This is consistent with a less favorable formation of three linked five-membered chelate rings around the larger Pt(II) ion. The ^{195}Pt-^{15}N NMR coupling constants and the ^{195}Pt chemical shifts also provide evidence for this effect. The use of ^{195}Pt NMR in conjunction with ^{15}N-substituted ligands provides an excellent method to characterize the peptide complexes that are slow to equilibrate in solution.

Acknowledgment. This investigation was supported by Public Health Service Grant No. GM12152 from the National Institute of General Medical Sciences. We are grateful to Robert E. Santini for his assistance in the NMR experiments.

(38) Dukes, G. R.; Margerum, D. W. *J. Am. Chem. Soc.* **1972**, *94*, 8414-8420.

Contribution from the Department of Chemistry, Purdue University, West Lafayette, Indiana 47907

Stepwise Hydrolysis Kinetics of Tetrachloroplatinate(II) in Base

Li Wu, Brigitte E. Schwederski, and Dale W. Margerum*

Received January 26, 1990

The stepwise hydrolysis of tetrachloroplatinate(II) in basic solution is investigated by ^{195}Pt NMR spectroscopy. Four sequential reactions are observed when 0.05 M $PtCl_4^{2-}$ is reacted with 1.0 M NaOH:

$$PtCl_4^{2-} \xrightarrow[k_1]{OH^-} PtCl_3(OH)^{2-} \xrightarrow[k_2]{OH^-} cis\text{-}PtCl_2(OH)_2^{2-} \xrightarrow[k_3]{OH^-} PtCl(OH)_3^{2-} \xrightarrow[k_4]{OH^-} Pt(OH)_4^{2-}$$

The reactions are not reversible, and the individual pseudo-first-order rate constants (s^{-1}, 25 °C, μ = 1.15 M) are as follows: $k_1 = 6.6 \times 10^{-5}$, $k_2 = 8 \times 10^{-5}$, $k_3 = 3.3 \times 10^{-6}$, $k_4 = 2.2 \times 10^{-6}$. The hydroxide ion concentration dependence for the first reaction, corrected to μ = 0.50 M, gives $k_1^{corr} = k_1^{H_2O} + k_1^{OH}[OH^-]$, where $k_1^{H_2O}$ is 3.6×10^{-5} s^{-1} and k_1^{OH} is 3.7×10^{-5} M^{-1} s^{-1}. The UV-vis spectrum of each Pt(II) species is resolved from repetitive scans on the basis of the NMR-determined rate constants. Dissolved O_2 (1 atm pressure) in 0.8 M OH^- converts $Pt(OH)_4^{2-}$ to $Pt(OH)_6^{2-}$ with a pseudo-first-order rate constant of 3×10^{-5} s^{-1}.

Introduction

Although the stepwise acid hydrolysis of tetrachloroplatinate(II) in aqueous acidic solution has been well studied,[1-12] much less is known about the hydrolysis of this complex in basic solution. Previous papers[2,3] reported only the kinetics of substitution for the first chloride ion. In hydroxide concentrations up to 0.1 M,[2,3] the proposed rate-determining step is the replacement of chloride ion by water (eq 1) followed by a rapid neutralization with hydroxide ion (eq 2).

$$PtCl_4^{2-} + H_2O \rightarrow PtCl_3(H_2O)^- + Cl^- \quad (1)$$

$$PtCl_3(H_2O)^- + OH^- \rightleftharpoons PtCl_3(OH)^{2-} + H_2O \quad (2)$$

Our investigation of the base hydrolysis of $PtCl_4^{2-}$ by ^{195}Pt NMR spectroscopy shows that four sequential reactions take place (eq 3). The rate constants are all larger than predicted from the

$$PtCl_4^{2-} \xrightarrow[k_1]{OH^-} PtCl_3(OH)^{2-} \xrightarrow[k_2]{OH^-} cis\text{-}PtCl_2(OH)_2^{2-} \xrightarrow[k_3]{OH^-} PtCl(OH)_3^{2-} \xrightarrow[k_4]{OH^-} Pt(OH)_4^{2-} \quad (3)$$

acid hydrolysis values,[11] and k_1 shows a hydroxide dependence in high base concentrations (≥0.5 M). The reactions are not

(1) Grantham, L. F.; Elleman, T. S.; Martin, D. S., Jr. *J. Am. Chem. Soc.* **1955**, *77*, 2965-2971.
(2) Banerjea, D.; Basolo, F.; Pearson, R. G. *J. Am. Chem. Soc.* **1957**, *79*, 4055-4062.
(3) Grinberg, A. A.; Kukushkin, Y. N. *Zh. Neorg. Khim.* **1957**, *2*, 2360-2367; **1961**, *6*, 306.
(4) Sanders, C. I.; Martin, D. S., Jr. *J. Am. Chem. Soc.* **1961**, *83*, 807-810.
(5) Colvin, C. B. Ph.D. Thesis, Iowa State University, Ames, IA, 1962.
(6) Elding, L. I.; Leden, I. *Acta Chem. Scand.* **1966**, *20*, 706-715.
(7) Elding, L. I. *Acta Chem. Scand.* **1966**, *20*, 2559-2567.
(8) Drougge, L.; Elding, L. I.; Gustafson, L. *Acta Chem. Scand.* **1967**, *21*, 1647-1653.
(9) Elding, L. I. *Acta Chem. Scand.* **1970**, *24*, 1331-1340.
(10) Elding, L. I. *Acta Chem. Scand.* **1970**, *24*, 1341-1354.
(11) Elding, L. I. *Acta Chem. Scand.* **1970**, *24*, 1527-1540.
(12) Elding, L. I. *Inorg. Chim. Acta* **1978**, *28*, 255-262.

0020-1669/90/1329-3578$02.50/0

Table I. Spin-Lattice Relaxation Times of $PtCl_x(OH)_{4-x}^{2-}$ Complexes[a]

complex	T_1, s	complex	T_1, s
$PtCl_4^{2-}$	0.113 ± 0.004	$PtCl(OH)_3^{2-}$	0.048 ± 0.006
$PtCl_3(OH)^{2-}$	0.12 ± 0.03	$Pt(OH)_4^{2-}$	0.074 ± 0.008
cis-$PtCl_2(OH)_2^{2-}$	0.071 ± 0.002		

[a] Conditions: $[Pt]_T$ = 0.07 M, 1.0 M NaOH, 25 ± 2 °C, 200 MHz.

reversible under our experimental conditions.

The ultraviolet–visible spectra of the five complexes in eq 3 overlap each other, so that it is very difficult to resolve the individual hydrolysis steps. On the other hand, ^{195}Pt NMR spectroscopy gives well-separated chemical shifts for the various $PtCl_x(H_2O)_{4-x}^{2-x}$ species.[13,14] We find similar incremental chemical shifts for the $PtCl_x(OH)_{4-x}^{2-}$ series that permit the individual concentrations to be monitored by ^{195}Pt NMR spectroscopy. Some of the reactions are slow, and spectra are collected over a 10-day period without disturbing the position of the NMR tube. This allows the evaluation of the k_1, k_2, k_3, and k_4 rate constants when $[OH^-]_{init}$ is 1.0 M. The same reaction conditions are studied by repetitive UV–vis spectral scans, and the NMR-evaluated rate constants are used to resolve the UV–vis spectrum for each Pt(II) species. Variation of the initial NaOH concentration from 0.50 to 2.20 M shows that the rate of $PtCl_4^{2-}$ hydrolysis depends on the hydroxide concentration.

Experimental Section

Reagents. Potassium tetrachloroplatinate(II) (K_2PtCl_4) was obtained from Strem Chemicals. Stock solutions of NaOH were prepared from analytical grade material and standardized by titration with potassium hydrogen phthalate to the phenolphthalein end point.

NMR Measurements. ^{195}Pt FT-NMR spectra were measured with a Varian XL-200 NMR spectrometer with a 10-mm broad-band probe at 42.917 MHz. The spectra were run in aqueous solutions and were proton decoupled by using the Waltz-16 decoupler method. A typical experiment with 0.05 M $[Pt]_T$ used 0.15-s acquisition time, 0.20-s delay time, and 10000 transients collected over a period of 1 h. The pulse width was 15 μs, and the pulse angle was 59°. Each spectrum contained 15000 data points for a 50000-Hz window. This gave signal-to-noise (S/N) ratios greater than 20. The temperature was controlled with air flow from an Igersoll-Rand Type 31 compressor to a refrigerated air cooler and a heat exchanger.[15] The sample air temperature was measured with a Doric Series 400-A digital thermometer. The temperature within the NMR probe was 25 ± 2 °C. (The temperature was calibrated with 100% CH_3OH under identical conditions.) All NMR chemical shifts are reported positive to lower shielding. ^{195}Pt NMR spectral lines are referenced to an external standard of Na_2PtCl_6 in 1 M HCl.[16] Absolute frequencies are used to calculate chemical shifts. The frequencies for the XL-200 spectrometer are referred to a single master oscillator with an absolute accuracy of better than 5 parts in 10^9 on a long-term basis.

Spin–Lattice Relaxation Times. T_1 values of the complexes $PtCl_x(OH)_{4-x}^{2-}$ were determined by the inversion recovery method (the standard 180°–τ–90° pulse sequence).[17] A reaction solution of $[Pt]_T$ = 0.07 M was prepared by dissolving K_2PtCl_4 in 1.0 M NaOH, which was previously deoxygenated. To ensure that the solutions were O_2-free, Ar gas was bubbled through the solution for another 20 min prior to the NMR measurements. T_1 measurements for each complex were carried out when the complex was near its maximum concentration during the reaction. To optimize the results, each T_1 was measured where the complex peak was at its resident frequency by selecting different transmitter offset (TO) values. A spectral window of 1000 Hz was used for these measurements. At least 500 transients were collected for S/N > 10. T_1 values for the complexes range from 0.048 to 0.12 s (Table I). The values are small, which permits the assumption that the intensity of each complex peak is directly proportional to its concentration. Therefore, the peak height of each species in the ^{195}Pt NMR spectrum was used as a measure of its concentration.

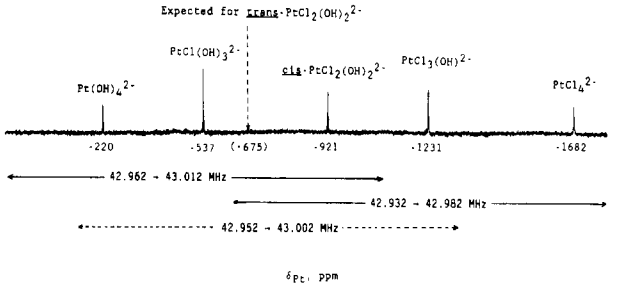

Figure 1. ^{195}Pt NMR spectra of $PtCl_x(OH)_{4-x}^{2-}$ complexes. Singals of $PtCl_4^{2-}$ and $PtCl_3(OH)^{2-}$ were observed with a center frequency of 42.957 MHz, and spectra were collected after 3.5 h. (The signal of *cis*-$PtCl_2(OH)_2^{2-}$ was also observed in this window, but is not shown in this figure.) Peaks of *cis*-$PtCl_2(OH)_2^{2-}$, $PtCl(OH)_3^{2-}$, and $Pt(OH)_4^{2-}$ were observed in another window with a center frequency of 42.987 MHz after 80 h. A third window with a center frequency of 42.977 MHz was used to confirm the absence of *trans*-$PtCl_2(OH)_2^{2-}$.

Table II. ^{195}Pt NMR Chemical Shifts for $PtCl_x(OH)_{4-x}^{2-}$ and $PtCl_x(H_2O)_{4-x}^{2-x}$ Complexes

Pt(II) complex[a]	^{195}Pt NMR chem shift, ppm L = OH^-[b]	L = H_2O[c]	Pt(II) complex[a]	^{195}Pt NMR chem shift, ppm L = OH^-[b]	L = H_2O[c]
$PtCl_4$	−1682		*trans*-$PtCl_2L_2$	−675[d]	−644
$PtClL_3$	−1231	−1185	$PtClL_3$	−537	−350
cis-$PtCl_2L_2$	−921	−811	PtL_4	−220	+31[d]

[a] Charges are omitted. [b] This work. [c] Appleton, T. G.; Hall, J. R.; Ralph, S. F.; Thompson, C. S. *Inorg. Chem.* **1984**, *23*, 3521–3525. [d] Gröning, Ö.; Drakenberg, T.; Elding, L. I. *Inorg. Chem.* **1982**, *21*, 1820–1824.

A T_1 value of 0.46 s for a 100 MHz instrument has been reported[18] for $PtCl_4^{2-}$. Since T_1 values are inversely proportional to the square of the field,[19] this value is in good agreement with our measurement of T_1 = 0.113 s for this complex with a 200-MHz instrument.

Base Hydrolysis of $PtCl_4^{2-}$. The reaction solutions of 0.05 M $PtCl_4^{2-}$ in 1.0 M NaOH were flushed with argon. A 10-day experiment was designed in order to follow the changes of concentrations of all five complexes involved in the reaction. The position of the NMR tube and the setting of the instrument were not disturbed during this period. Since the maximum spectral window of the instrument is 50000 Hz (1200 ppm), while the signals of the complexes are found over a range of 1500 ppm, two different spectral windows were used in this experiment. Signals of $PtCl_4^{2-}$, $PtCl_3(OH)^{2-}$, and *cis*-$PtCl_2(OH)_2^{2-}$ were seen in one window (with a center frequency of 42.957 MHz), in which spectra were collected during the first 34 h. Peaks of *cis*-$PtCl_2(OH)_2^{2-}$, $PtCl(OH)_3^{2-}$, and $Pt(OH)_4^{2-}$ were observed in another window (with a center frequency of 42.987 MHz), for the next 200 h.

UV–Vis Spectra. A Perkin-Elmer 320 spectrophotometer equipped with a PE 3600 data station was used to obtain multiple scans of spectra (1.00-cm cell) for the reaction system at 25.0 ± 0.1 °C over a 12-day period. The reaction solution with $[Pt]_T = 9.30 \times 10^{-3}$ M and $[OH^-]$ = 1.00 M was deoxygenated by flushing argon through it before spectra were taken.

Data Analysis. In the kinetic studies each ^{195}Pt NMR spectrum took 1 h to collect. The intensities were used as the measure of the concentration, and the midpoint of the time interval was used as the reaction time. Since the signal in the obtained spectrum is actually the integrated average during that time period, it is not quite equal to the intensity at the midpoint. However, this discrepancy introduces less than 1% error for the fastest reaction. The validity of using the midpoint as the time measure is given in the Appendix.

Experimental data were analyzed by a nonlinear regression curve-fitting program, CURVE,[20] that uses a Marquardt algorithm.

(13) Gröning, Ö.; Elding, L. I. *Inorg. Chem.* **1989**, *28*, 3366–3372.
(14) Appleton, T. G.; Hall, J. R.; Ralph, S. F.; Thompson, C. S. M. *Inorg. Chem.* **1984**, *23*, 3521–3525.
(15) (a) Allerhand, A. A.; Addleman, R. E.; Osman, D.; Dohrenwend, M. *J. Magn. Reson.* **1985**, *65*, 361–363. (b) Allerhand, A. A.; Addleman, R. E.; Osman, D. *J. Am. Chem. Soc.* **1985**, *107*, 5809–5810.
(16) Kerrison, S. J. S.; Sadler, P. J. *J. Magn. Reson.* **1978**, *31*, 321–325.
(17) (a) Vold, R. L.; Waugh, J. S.; Klein, M. P.; Phelps, D. E. *J. Chem. Phys.* **1968**, *48*, 3831–3832. (b) Freeman, R.; Hill, H. D. W. *J. Chem. Phys.* **1969**, *51*, 3140–3141.
(18) Pesek, J. J.; Mason, W. R. *J. Magn. Reson.* **1977**, *25*, 519–529.
(19) Abragam, A. *The Principles of Nuclear Magnetism*; Clarendon Press: U.K., Oxford, 1983; p 406.
(20) Wang, Y. L. Ph.D. Thesis, Purdue University, West Lafayette, IN, 1989.

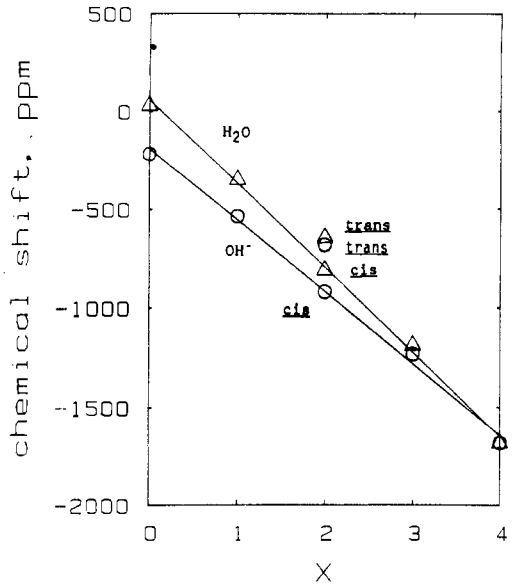

Figure 2. Additivity of chemical shifts of the ^{195}Pt NMR spectra for $PtCl_x(OH)_{4-x}^{2-}$ and $PtCl_x(H_2O)_{4-x}^{2-x}$: OH^-, slope = −362 ppm, intercept = −195 ppm; H_2O, slope = −426 ppm, intercept = 50 ppm.

Results and Discussion

^{195}Pt NMR Spectrum of $PtCl_x(OH)_{4-x}^{2-}$ Complexes. Five peaks were found in the ^{195}Pt NMR spectrum of an aged solution of K_2PtCl_4 in 1 M base (Figure 1). These peaks are assigned to the various species $PtCl_x(OH)_{4-x}^{2-}$ by comparison to the ^{195}Pt NMR spectra of their aquo analogues,[13,14] $PtCl_x(H_2O)_{4-x}^{2-x}$ (Table II). The only $PtCl_2(OH)_2^{2-}$ complex found in our experiments at −921 ppm is assigned to the cis complex. Figure 1 indicates the expected δ_{Pt} location for the trans complex at −675 ppm,[21] but we found no detectable signal at this chemical shift. The kinetic trans effect predicts preferential formation of the *cis*-$PtCl_2(OH)_2^{2-}$ complex. Figure 2 shows that plots of δ_{Pt} vs the number of Cl^- ions present in the complexes are linear for both the $PtCl_x(OH)_{4-x}^{2-}$ and $PtCl_x(H_2O)_{4-x}^{2-x}$ series. The *cis*-$PtCl_2(H_2O)_2$ and *cis*-$PtCl_2(OH)_2^{2-}$ complexes fall on the linear relationship, while the *trans*-$PtCl_2(H_2O)_2$ and *trans*-$PtCl_2(OH)_2^{2-}$ complexes fall off the line.

The least-squares line in Figure 2 for the $PtCl_x(OH)_{4-x}^{2-}$ complexes is $\delta_{Pt} = -195 - 362x$. Thus the value of the ^{195}Pt chemical shift is additive for each substitution of Cl^- by OH^-. Similar additivities are seen in Figure 2 for H_2O[13,14] and are also found for the substitution of Cl^- or OH^- for NH_3 in complexes of $Pt(NH_3)_xL_{4-x}$.[22]

Nonreversibility of the Reaction. The ^{195}Pt NMR spectra during the reaction period show complete loss of $PtCl_4^{2-}$ and of $PtCl_3(OH)^{2-}$, while 90% of *cis*-$PtCl_2(OH)_2^{2-}$ is lost in 10 days. Equilibrium constants for the substitution of hydroxide ions in $Pt(OH)_4^{2-}$ by chloride ions (eq 4) were measured potentiometrically,[23] with values of $pK_1 = 10.5$, $pK_2 = 10.0$, $pK_3 = 9.5$, and $pK_4 = 8.7$. On the basis of these constants and $pK_w = 13.79$,[24] equilibrium constants for the base hydrolysis of $PtCl_4^{2-}$ (eq 5) were calculated to be $K_1' = 1.2 \times 10^5$, $K_2' = 2.0 \times 10^4$, $K_3' = 6.2 \times 10^3$, and $K_4' = 2.0 \times 10^3$. These equilibrium constants are sufficiently large to cause each step of the reaction sequence to be essentially irreversible under our experimental conditions.

$$PtCl_{n-1}(OH)_{5-n}^{2-} + H^+ + Cl^- \underset{}{\overset{K_n}{\rightleftharpoons}} PtCl_n(OH)_{4-n}^{2-} + H_2O \quad (4)$$
$$n = 1\text{–}4$$

$$PtCl_n(OH)_{4-n}^{2-} + OH^- \overset{K_{5-n}'}{\rightleftharpoons} PtCl_{n-1}(OH)_{5-n}^{2-} + Cl^- \quad (5)$$
$$n = 4\text{–}1$$

(21) Gröning, Ö.; Drakenberg, T.; Elding, L. I. *Inorg. Chem.* **1982**, *21*, 1820–1824.
(22) Appleton, T. G.; Hall, J. R.; Ralph, S. F. *Inorg. Chem.* **1985**, *24*, 4685–4693.
(23) Peshchevitskii, B. I.; Ptitsyn, B. V.; Leskova, N. M. *Izv. Sibirsk. Otd. Akad. Nauk SSSR* **1962**, *11*, 143–145. (Cited in: *Stability Constants*; The Chemical Society: London, 1964; p 284.)
(24) Smith, R. M.; Martell, A. E. *Critical Stability Constants*; Plenum Press: New York, 1976; Vol. 4, p 1.

Table III. Rate Constants for the Consecutive Hydrolysis Reactions of $PtCl_4^{2-}$ in Base[a] and in Acid Solutions[b]

Base

reactant	$[OH^-]_{av}$, M	rate const, s^{-1}
$PtCl_4^{2-}$	0.95	$k_1 = (6.6 \pm 0.7) \times 10^{-5}$
$PtCl_3(OH)^{2-}$	0.94	$k_2 = (8 \pm 1) \times 10^{-5}$
cis-$PtCl_2(OH)_2^{2-}$	0.86	$k_3 = (3.3 \pm 0.1) \times 10^{-6}$
$PtCl(OH)_3^{2-}$	0.86	$k_4 = (2.2 \pm 0.1) \times 10^{-6}$

Acid

reactant	$[H^+]$, M	rate const, s^{-1}
$PtCl_4^{2-}$	0.50	$k_1' = (3.6 \pm 0.3) \times 10^{-5}$ [c]
$PtCl_3(H_2O)^-$	0.50	$k_2' = (5 \pm 1) \times 10^{-5}$ [c]
cis-$PtCl_2(H_2O)_2$	0.50	$k_3' = (2 \pm 2) \times 10^{-7}$ [c]
$PtCl(H_2O)_3^+$	0.50	$k_4' = (2.8 \pm 0.7) \times 10^{-7}$ [d]

[a] $[Pt]_T = 0.050$ M, $[OH^-]_{init} = 1.00$ M, 25 ± 2 °C, $\mu = 1.15$ M. [b] 25.0 ± 0.1 °C, $\mu = 0.50$ M ($HClO_4$). In aqueous acidic solution, the reaction is reversible. Only the rate constants of the forward (hydrolysis) reactions are listed. [c] Elding, L. I. *Acta Chem. Scand.* **1970**, *24*, 1341–1354. [d] Elding, L. I. *Inorg. Chim. Acta* **1978**, *28*, 255–262.

Rate Constants. Data from the ^{195}Pt NMR intensities vs time for each complex in eq 3 were analyzed by use of the four-step pseudo-first-order consecutive reaction model given in eq 6–11.

$$A \xrightarrow{k_1} B \xrightarrow{k_2} C \xrightarrow{k_3} D \xrightarrow{k_4} E \quad (6)$$

$$[A] = [A]_0 e^{-k_1 t} \quad (7)$$

$$[B] = \frac{k_1[A]_0}{k_2 - k_1}(e^{-k_1 t} - e^{-k_2 t}) \quad (8)$$

$$[C] = k_1 k_2 [A]_0 \left[\frac{e^{-k_1 t}}{(k_2 - k_1)(k_3 - k_1)} + \frac{e^{-k_2 t}}{(k_1 - k_2)(k_3 - k_2)} + \frac{e^{-k_3 t}}{(k_1 - k_3)(k_2 - k_3)} \right] \quad (9)$$

$$[D] = k_1 k_2 k_3 [A]_0 \left[\frac{e^{-k_1 t}}{(k_2 - k_1)(k_3 - k_1)(k_4 - k_1)} + \frac{e^{-k_2 t}}{(k_1 - k_2)(k_3 - k_2)(k_4 - k_2)} + \frac{e^{-k_3 t}}{(k_1 - k_3)(k_2 - k_3)(k_4 - k_3)} + \frac{e^{-k_4 t}}{(k_1 - k_4)(k_2 - k_4)(k_3 - k_4)} \right] \quad (10)$$

$$[E] = [A]_0 \left[1 - \frac{k_2 k_3 k_4 e^{-k_1 t}}{(k_2 - k_1)(k_3 - k_1)(k_4 - k_1)} - \frac{k_1 k_3 k_4 e^{-k_2 t}}{(k_1 - k_2)(k_3 - k_2)(k_4 - k_2)} - \frac{k_1 k_2 k_4 e^{-k_3 t}}{(k_1 - k_3)(k_2 - k_3)(k_4 - k_3)} - \frac{k_1 k_2 k_3 e^{-k_4 t}}{(k_1 - k_4)(k_2 - k_4)(k_3 - k_4)} \right] \quad (11)$$

The high concentration of Pt(II) (0.05 M) that is needed for the NMR measurements causes some decrease in the hydroxide ion concentration as the various $PtCl_x(OH)_{4-x}^{2-}$ species are formed. The percent change of $[OH^-]$ for each hydrolysis step is small relative to the precision of the measurements, so the assumption that the reactions are pseudo first order is valid. Table III gives the calculated $[OH^-]_{av}$ for each rate constant, based on the change in concentrations of the $PtCl_x(OH)_{4-x}^{2-}$ species during the time interval used to evaluate this rate constant. Figure 3 shows the experimental points for the fraction of each complex present as a function of time.

The k_1 value, obtained by linear regression analysis from data taken from 1 to 10 h, is $(6.6 \pm 0.7) \times 10^{-5}$ s^{-1}. The $[OH^-]$ varies

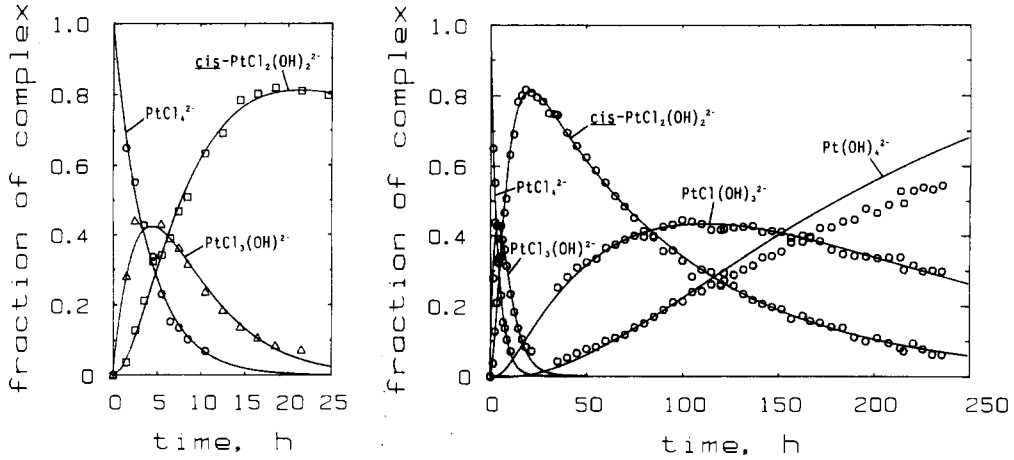

Figure 3. ^{195}Pt NMR data for changes of concentrations of Pt(II) complexes during the hydrolysis reaction with 1.00 M NaOH at 25 ± 2 °C: (a, left) TO setting = 40 000; (b, right) TO setting = 70 000. Curves are fitted from eqs 6–11.

from 0.98 to 0.92 M during this time because some *cis*-$PtCl_2(OH)_2^{2-}$ as well as $PtCl_3(OH)^{2-}$ is formed. In acid, the hydrolysis rate constant[7] (independent of $[H^+]$) is $(3.6 \pm 0.3) \times 10^{-5}$ s^{-1}, so the hydrolysis rate in base has both a solvent and a $[OH^-]$ term. Hence, the ±3% change of $[OH^-]$ during the reaction will cause only at ±1.5% change in the observed k_1 value.

The k_2 rate constant was evaluated from changes in the $PtCl_3(OH)^{2-}$ concentration from 1 to 20 h ($[OH^-]$ varies from 0.98 to 0.90 M) by using eq 8 and the CURVE[20] program.

The k_3 rate constant was evaluated from changes in the *cis*-$PtCl_2(OH)_2^{2-}$ concentration for data collected from 30 to 240 h. This permitted a single NMR window to be used. Since the concentrations of $PtCl_4^{2-}$ and $PtCl_3(OH)^{2-}$ are both negligible over 30 h, a linear regression analysis can be used to evaluate k_3 as $(3.28 \pm 0.04) \times 10^{-6}$ s^{-1}. During this time interval the calculated $[OH^-]$ varies by ±4% (from 0.89 to 0.82 M), so the actual precision of the k_3 rate constant is probably less than given above. The k_4 rate constant was evaluated from changes in the $PtCl(OH)_3^{2-}$ concentration from 30 to 240 h by using eq 10 and the CURVE program. Figure 3 shows the fit of the rate constants to the experimental data. The deviation after 120 h between the calculated curve and the experimental data for $Pt(OH)_4^{2-}$ is caused by the formation of the Pt(IV) complex, $Pt(OH)_6^{2-}$. Hence the evaluation of k_4 is based on the loss of $PtCl(OH)_3^{2-}$.

A k_2 value of 3.5×10^{-5} s^{-1} in 0.10 M $[OH^-]$ was estimated by Colvin.[5] He proposed a mechanism similar to eq 1 and 2, where water first reacts with $PtCl_3(OH)^{2-}$ followed by the neutralization of the aquo product. Our value for k_2 of $(8 \pm 1) \times 10^{-5}$ s^{-1} in 0.94 M OH^- is significantly larger, which suggests some contribution from a direct OH^- substitution path such as we observed for k_1. However, the large uncertainty in our k_2 determination makes it difficult to evaluate the $[OH^-]$ dependence of the second step in the hydrolysis. The UV–vis spectral method used by Colvin has even greater uncertainties in the evaluation of k_2.

Reaction between O_2 and $Pt(OH)_4^{2-}$. Although NMR spectra were taken after flushing argon through the reaction solution to remove oxygen, a very low but significant signal at +3396 ppm was found in the 10-day-old solution. This peak has been assigned to $Pt(OH)_6^{2-}$, which Appleton et al.[22] observed from the disproportionation of $Pt(OH)_4^{2-}$, when [Pt(II)] was greater than 0.05 M (eq 12). We also observed the formation of black metallic

$$2Pt(OH)_4^{2-} \rightarrow Pt^0 + Pt(OH)_6^{2-} + 2OH^- \qquad (12)$$

precipitates in solutions of $[Pt(II)] \geq 0.07$ M in 1 M NaOH. Since we could not find evidence for any metallic platinum in the 10-day NMR experiment, we believe that the appearance of $Pt(OH)_6^{2-}$ was due to oxidation by traces of oxygen that leaked into the NMR tube. The same 10-day-old reaction solution was saturated with oxygen gas, in order to see how rapidly $Pt(OH)_6^{2-}$ would form (eq 13). The appearance of the $Pt(OH)_6^{2-}$ signal during the redox

$$Pt(OH)_4^{2-} + \tfrac{1}{2}O_2 + H_2O \rightarrow Pt(OH)_6^{2-} \qquad (13)$$

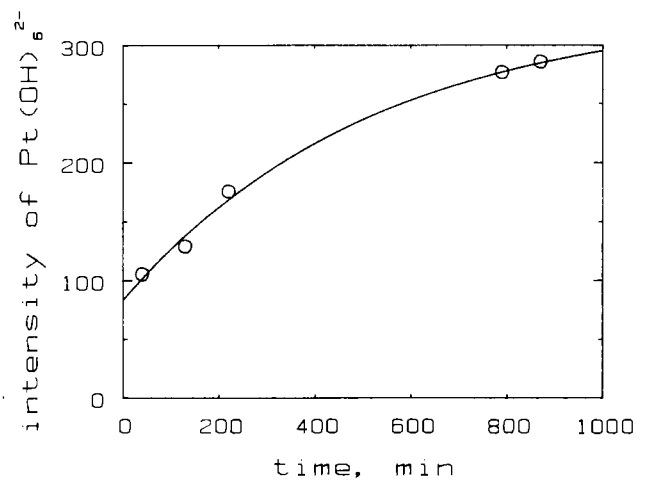

Figure 4. Appearance of $Pt(OH)_6^{2-}$ in the reaction between $Pt(OH)_4^{2-}$ and O_2. $[Pt(OH)_4^{2-}] \simeq 0.04$ M; $P(O_2) = 1$ atm; $T = 25 \pm 2$ °C. The time axis starts with the time of NMR measurement, and the intercept value of 84 indicates oxidation of $Pt(OH)_4^{2-}$ during the kinetic measurement of the base hydrolysis of $PtCl_4^{2-}$ and during the period that oxygen gas was bubbled through the aged reaction solution. The curve shows the fit of a pseudo-first-order rate constant of $(3 \pm 1) \times 10^{-5}$ s^{-1}.

reaction is shown in Figure 4. The pseudo-first-order rate constant of the redox reaction is $(3 \pm 1) \times 10^{-5}$ s^{-1}, when the pressure of oxygen is 1 atm (the dissolved O_2 concentration is 8.34×10^{-4} M under 1 atm of oxygen pressure in 1 M NaOH solution).[25] About 60 h after oxygen was bubbled through the solutions, the $Pt(OH)_4^{2-}$ NMR peak had disappeared, but there was still an appreciable amount of $PtCl(OH)_3^{2-}$ left in the reaction solution. This indicates that $PtCl(OH)_3^{2-}$ is not as easily oxidized as is $Pt(OH)_4^{2-}$.

Trans Effect. Hydroxide ion has a smaller trans effect than chloride ion.[26,27] This accounts for the fact that the k_1 and k_2 rate constants, for species where Cl^- is in a position trans to the displaced Cl^-, are more than an order of magnitude larger than the k_3 and k_4 rate constants.

The trans effect also predicts that the hydrolysis of $PtCl_3(OH)^{2-}$ should give *cis*-$PtCl_2(OH)_2^{2-}$ in preference to *trans*-$PtCl_2(OH)_2^{2-}$. We were not able to observe any trans species in the ^{195}Pt NMR experiments. Since we would also expect *trans*-$PtCl_2(OH)_2^{2-}$ to hydrolyze faster than *cis*-$PtCl_2(OH)_2^{2-}$ to give $PtCl(OH)_3^{2-}$, it is possible that both hydrolysis pathways exist and the trans species

(25) Seidell, A. In *Solubilities—Inorganic and Metal-Organic Compounds*, 4th ed.; Linke, W. F., Ed.; American Chemical Society: Washington, DC, 1965; Vol. 2, p 1230.
(26) Basolo, F. *Adv. Chem. Ser.* **1965**, *49*, 81–106.
(27) Langford, C. H.; Gray, H. B. *Ligand Substitution Processes*; Benjamin: New York, 1965; p 24.

Table IV. Effect of Hydroxide Ion Concentration and Ionic Strength on the Hydrolysis of $PtCl_4^{2-}$ [a]

$[OH^-]_{av}$, M	μ, M	$k/k_{0.5}$ [b]	$10^5 k_1^{obsd}$, s^{-1}	$10^5 k_1^{cor}$, s^{-1} [b]
0	0.50	1	3.6	3.6[c]
0.45	0.60	1.0	5.4	5.4
0.95	1.10	0.86	6.6	7.1
1.43	1.58	0.65	7.2	9.1
1.45	1.60	0.65	7.1	9.0
1.67	1.82	0.56	6.7	9.2
1.88	2.03	0.48	7.1	10.9
2.15	2.30	0.39	6.8	11.8

[a] Conditions: $[Pt]_T$ = 0.05 M, 25 ± 2 °C. [b] The salt effect is corrected to μ = 0.50 M by the Debye–Hückel–Brønsted–Davies relationship (eq 16), b = 0.22. [c] Elding, L. I. *Acta Chem. Scand.* **1966**, *20*, 2559–2567.

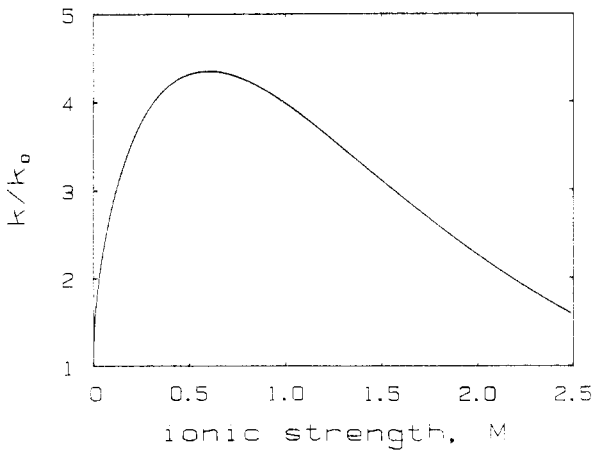

Figure 5. Ionic strength effect on the rate constant based on the Debye–Hückel–Brønsted–Davies relationship (eq 16) with $Z_A = -2$, $Z_B = -1$, and b = 0.22.

is present in very low concentrations. This situation was observed by Elding[28] in the acid hydrolysis of $PtCl_4^{2-}$. We tested the fit of the experimental data by addition of a second hydrolysis pathway with a steady-state concentration of *trans*-$PtCl_2(OH)_2^{2-}$. This did not give an improved fit for the rate of loss of $PtCl_3(OH)^{2-}$ and rate of formation of $PtCl(OH)_3^{2-}$, so the contribution of a trans pathway is not appreciable.

$[OH^-]$ Dependence of k_1. The hydrolysis rate constant for $PtCl_4^{2-}$ in acid solutions is 3.6 × 10^{-5} s^{-1} (μ = 0.5 M, 25.0 °C),[7] while the k_1 value in 0.95 M $[OH^-]$ is 6.6 × 10^{-5} s^{-1}. The solvent pathway in eq 1 and 2 makes a sizable contribution to the rate of formation of $PtCl_3(OH)^{2-}$, but a direct OH^- pathway also exists (eq 14). A two-term rate expression is typical for square-planar

$$PtCl_4^{2-} + OH^- \xrightarrow{k_1^{OH}} PtCl_3(OH)^{2-} + Cl^- \qquad (14)$$

substitution reactions and the observed k_1 value is expected to be the sum of these two pathways (eq 15). Table IV gives the k_1^{obsd}

$$k_1^{obsd} = k_1^{H_2O} + k_1^{OH}[OH^-] \qquad (15)$$

values as $[OH^-]$ varies from 0 to 2.15 M. The k_1^{obsd} values increase by a factor of 2 as $[OH^-]$ increases. Previous tests of the effect of hydroxide ion used 0.1 M or less OH^-, which was too low to give a significant contribution from the $k_1[OH^-]$ term in eq 15. The k_1^{obsd} values level off above 1.4 M OH^- because of the large variation of ionic strength (μ = 0.50–2.30 M). In this range the Debye–Hückel–Brønsted–Davies equation[29,30] (eq 16, where k_0

$$\log k = \log k_0 + 1.02 Z_A Z_B \left(\frac{\mu^{1/2}}{1 + \mu^{1/2}} - b\mu \right) \qquad (16)$$

is the rate constant at μ = 0) predicts a reversal of the normal

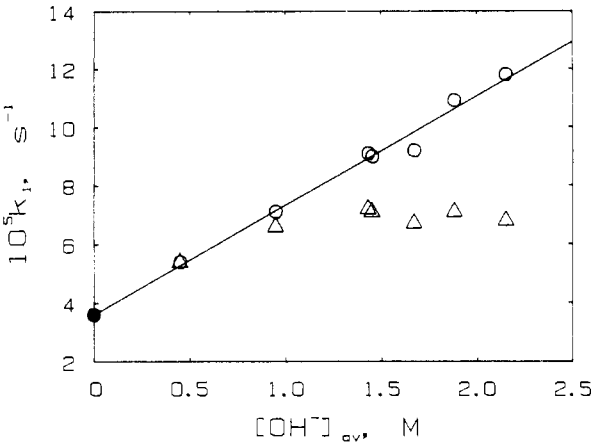

Figure 6. Hydroxide concentration dependence of the rate constant for the first step of the reaction sequence, k_1^{obsd}, at 25 ± 2 °C (△): (○) values corrected to 0.50 M ionic strength; (●) Elding's acid hydrolysis value at μ = 0.50 M.[7] Slope = (3.7 ± 0.2) × 10^{-5} M^{-1} s^{-1}; intercept = (3.6 ± 0.2) × 10^{-5} s^{-1}.

Table V. Ligand Nucleophilicities (n_{Pt}) and Second-Order Rate Constants (k_Y) for Substitution Reactions of $PtCl_4^{2-}$ [a]

ligand	n_{Pt}	k_Y, M^{-1} s^{-1}	ligand	n_{Pt}	k_Y, M^{-1} s^{-1}
H_2O	0.0	6.5 × 10^{-7} [b]	I^-	4.03	6.5 × 10^{-3}
OH^-	(1.6 ± 0.8)[c]	(3.7 ± 0.2) × 10^{-5} [d]	SCN^-	4.26	2.1 × 10^{-3}
			$SeCN^-$	5.71	0.53
NO_2^-	1.81	9 × 10^{-4}	thiourea	5.78	0.29
Br^-	2.79	1.78 × 10^{-3}	$S_2O_3^{2-}$	5.95	2.2 × 10^{-2}

[a] Cattalini, L.; Orio, A.; Nicolini, M. *J. Am. Chem. Soc.* **1966**, *88*, 5734–5738. [b] $k_1^{H_2O}/(55.5\ M\ H_2O)$. [c] This work, based on correlation with data for H_2O, Br^-, I^-, SCN^-, and $S_2O_3^{2-}$. [d] This work, calculated for μ = 0.50 M.

effect of ionic strength on reactants of the same sign ($Z_A = -2$, $Z_B = -1$), because of the influence of the interaction coefficient, b, at high ionic strength. The predicted ratio for k/k_0 as a function of μ is shown in Figure 5 when b = 0.22. The value of b is obtained from the best fit of eqs 15 and 16 (where k_1^{OH} is used for k) and is within the range of typical values for this interaction coefficient.[28,29] Figure 5 shows that the k/k_0 ratio is nearly constant from μ = 0.5 to 0.8 M and then decreases significantly as μ increases. Table IV gives k_1^{cor} values, which equal $k_1^{H_2O}$ (measured at μ = 0.50 M and assumed to be constant with change of μ) plus the k_1^{OH} values, which are normalized to μ = 0.50 M based on eq 16. Figure 6 shows plots of k_1^{obsd} (variable μ) and k_1^{cor} (0.50 M μ) against $[OH^-]_{av}$, where the slope for k_1^{OH} (μ = 0.50 M) equals (3.7 ± 0.2) × 10^{-5} M^{-1} s^{-1}. In 0.1 M NaOH (where μ = 0.1 M) the electrostatic repulsion between $PtCl_4^{2-}$ and OH^- becomes more important. We estimate that under these conditions the contribution from $k_1^{OH}[OH^-]$ should be only 0.2 × 10^{-5} s^{-1}, which is within the experimental error of the previous rate constant evaluations,[2,3] and explains why no hydroxide effect was seen previously.

Nucleophilicity (n_{Pt}) of OH^-. A set of nucleophilic reactivity constants, n_{Pt}, has been established[31] for Pt(II) substitution reactions based on eq 17, which is a variation of the Swain–Scott

$$\log k_Y = s(n_{Pt}) + \log k_S \qquad (17)$$

relationship.[32] Rate constants for OH^- substitution reactions of Pt(II) complexes have not been reported previously, although the lack of OH^- reactivity has led some authors[33a,34] to list the relative nucleophilicities as $Br^- > Cl^- > H_2O > OH^-$. In substitution

(28) Elding, L. I. *Inorg. Chim. Acta* **1978**, *31*, 243–250.
(29) Perlmutter-Hayman, B. *Prog. React. Kinet.* **1971**, *6*, 239–267.
(30) Pethybridge, A. D.; Pure, J. E. *Prog. Inorg. Chem.* **1972**, *17*, 327–389.
(31) Belluco, U.; Cattalini, L.; Basolo, F.; Pearson, R. G.; Turco, A. *J. Am. Chem. Soc.* **1965**, *87*, 241–246.
(32) Swain, C. G.; Scott, C. B. *J. Am. Chem. Soc.* **1953**, *75*, 141–147.
(33) Basolo, F.; Pearson, R. G. *Mechanisms of Inorganic Reactions*, 2nd ed.; Wiley: New York, 1967: (a) p 397; (b) p 67.
(34) Atwood, J. D. *Inorganic and Organometallic Reaction Mechanisms*; Brooks/Cole: Monterey, CA, 1985; p 60.

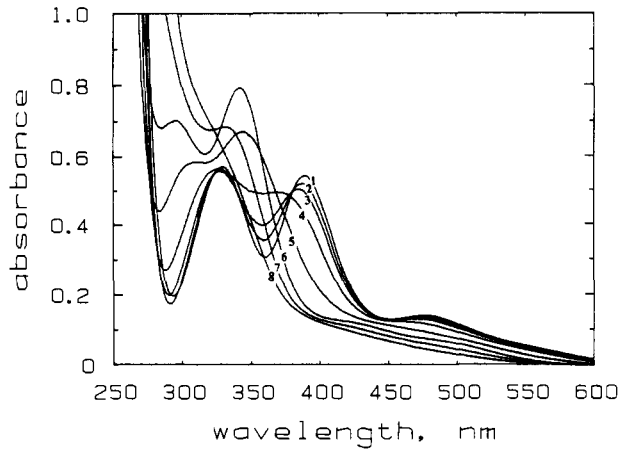

Figure 7. Multiple-scan UV-vis spectra of the reaction solution during the hydrolysis of $PtCl_4^{2-}$ in 1.00 M NaOH, at 25 ± 0.1 °C. Time intervals, h: (1) 0.5; (2) 1.5; (3) 2.5; (4) 5.5; (5) 14.5; (6) 39.2; (7) 118.2; (8) 228.7.

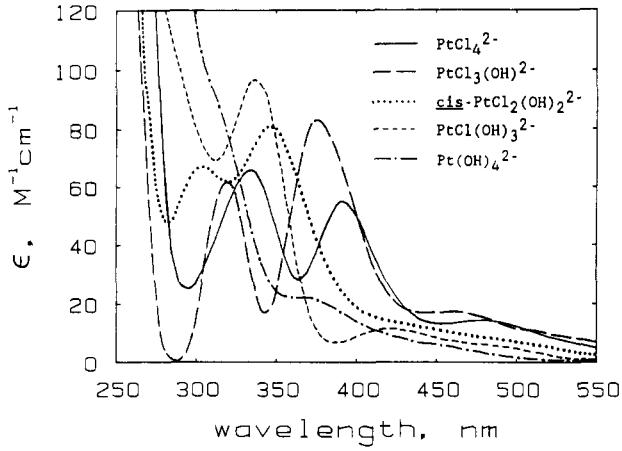

Figure 8. Resolved UV-vis spectra of the $PtCl_x(OH)_{4-x}^{2-}$ complexes.

reactions at carbon, the nucleophilicity (n) of OH^- is 4.20, which is greater than those of Cl^- (n = 3.04) or Br^- (n = 3.89).[35] However with Pt(II) substitutions, the softer nucleophiles have greater reactivity.[36] Our results show that for $PtCl_4^{2-}$ the relative order of nucleophilicity is $OH^- > H_2O$. Table V gives n_{Pt} values and second-order rate constants for various nucleophilic reactions with $PtCl_4^{2-}$. There is a considerable degree of scatter in the correlation, but Cattalini et al.[37] pointed out that the nucleophiles H_2O, Br^-, I^-, SCN^-, and $S_2O_3^{2-}$ follow the n_{Pt} scale, irrespective of the charge and nature of the complex. If we restrict the correlation to these values, we obtain the following for eq 17: log $k_S = -5.6 \pm 0.6$ and $s = 0.75 \pm 0.15$. Our k_1^{OH} rate constant of $(3.7 \pm 0.2) \times 10^{-5}$ M^{-1} s^{-1} then gives a value for the nucleophilicity of OH^-, $n_{Pt}^{OH} = 1.6 \pm 0.8$, based on statistical evaluation of both our rate constant and the uncertainties in the correlation equation. A previous estimate by Belluco et al.[31] gave $n_{Pt} \leq 1$ (based on values for CH_3OH and CH_3O^-), which falls within the lower range of our uncertainty. In any case, it appears that n_{Pt}^{OH} is much closer to 1 than to zero.

UV-Vis Spectra of $PtCl_x(OH)_{4-x}^{2-}$ Complexes. Fifty-six sets of UV-vis spectra of the reaction system were taken during a 12-day period. (Eight sets are shown in Figure 7.) On the basis of these spectra, a series of kinetic traces were derived, which were analyzed by using the CURVE program, and the rate constants determined by the ^{195}Pt NMR method, to resolve the molar absorptivities (ϵ) of various complexes at nearly 60 different wavelengths from 250 to 600 nm. Equation 18 gives the rela-

$$\frac{\text{Abs}}{b} = [\text{Pt}]_T\Bigg[\epsilon_E + (\epsilon_A - \epsilon_E)e^{-k_1t} + (\epsilon_B - \epsilon_E)k_1\frac{e^{-k_1t} - e^{-k_2t}}{k_2 - k_1} + (\epsilon_C - \epsilon_E)k_1k_2\Bigg(\frac{e^{-k_1t}}{(k_2 - k_1)(k_3 - k_1)} + \frac{e^{-k_2t}}{(k_1 - k_2)(k_3 - k_2)} + \frac{e^{-k_3t}}{(k_1 - k_3)(k_2 - k_3)}\Bigg) + (\epsilon_D - \epsilon_E)k_1k_2k_3\Bigg(\frac{e^{-k_1t}}{(k_2 - k_1)(k_3 - k_1)(k_4 - k_1)} + \frac{e^{-k_2t}}{(k_1 - k_2)(k_3 - k_2)(k_4 - k_2)} + \frac{e^{-k_3t}}{(k_1 - k_3)(k_2 - k_3)(k_4 - k_3)} + \frac{e^{-k_4t}}{(k_1 - k_4)(k_2 - k_4)(k_3 - k_4)}\Bigg)\Bigg] \quad (18)$$

tionship at each wavelength among the absorbance (Abs), the cell path (b), the molar absorptivities (ϵ) of species A through E, the rate constants, and time of reaction. Of course, some of the terms can be dropped at various times as indicated in Figure 3. The $[Pt(II)]_T$ was 9.3×10^{-3} M so that disproportionation did not occur, and the cuvette was sealed after Ar flushing to avoid any reaction with O_2. The resolved UV-vis spectra of five species are shown in Figure 8. The wavelengths for absorbance maxima (λ_{max}) and the related molar absorptivities for each of the complexes are listed in Table VI.

Table VI. Resolved UV-Vis Spectral Data for $PtCl_x(OH)_{4-x}^{2-}$ Complexes

species	complex	λ_{max}, nm (ϵ, M^{-1} cm^{-1})		
A	$PtCl_4^{2-}$	333 (66)	392 (55)	476 (14.6)
B	$PtCl_3(OH)^{2-}$	318 (61.5)	376 (83)	
C	*cis*-$PtCl_2(OH)_2^{2-}$	303 (67.5)	347 (81)	
D	$PtCl(OH)_3^{2-}$		337 (97)	420 (11.8)
E	$Pt(OH)_4^{2-}$		320 (75)[a]	

[a] Shoulder.

In Colvin's work,[5] the UV-vis spectra of $PtCl_3(OH)^{2-}$ and $PtCl_2(OH)_2^{2-}$ were reported and are in general agreement with our results. In his determination of the spectra, several solutions were prepared in aqueous medium and were allowed to reach equilibrium before NaOH was added. The spectra were taken immediately after addition of base. With the assumption that the time of the reaction of these aquo complexes with hydroxide was negligible during the time required to record a spectrum, the concentrations of the hydroxo complexes were assumed to be equal to the concentrations of the corresponding aquo complexes, which were calculated from equilibrium constants. The spectrum of each complex was then resolved. Colvin emphasized that uncertainties in the molar absorptivity values resulted because of the uncertainties in the equilibrium constants.

According to Elding's study of the UV-vis spectrum of K_2PtCl_4 in aqueous solution,[38] the peak at 333 nm for $PtCl_4^{2-}$ is assigned to a $d_{xy} \rightarrow d_{x^2-y^2}$ transition and the peak at 392 nm is assigned to the $d_{xz,yz} \rightarrow d_{x^2-y^2}$ transition, while the peak at 476 nm is associated with d-d singlet → triplet transitions. In the two spin-allowed d-d transitions, electrons move from symmetric orbitals (d_{xy}, $d_{xz,yz}$) into another symmetric orbital ($d_{x^2-y^2}$) and therefore are dipole-forbidden. In the case of $PtCl_4^{2-}$, the observation of these dipole-forbidden transitions is attributed to the chemical environment and the vibrations of the molecule that result in an asymmetric field around the complex.

The absorption bands shift to higher energy as the substitution reaction proceeds because OH^- is a stronger ligand field donor than Cl^-, as reflected in the spectrochemical series.[33b] The $d_{xz,yz} \rightarrow d_{x^2-y^2}$ transition changes from λ_{max} 392 nm for $PtCl_4^{2-}$ to 337 nm for $PtCl(OH)_3^{2-}$ (Table VI). The more asymmetric fields of $PtCl(OH)_3^{2-}$, *cis*-$PtCl_2(OH)_2^{2-}$, and $PtCl(OH)_3^{2-}$ appear to cause

(35) Hine, J. *Physical Organic Chemistry*, 2nd ed.; McGraw-Hill: New York, 1962; p 161.
(36) Pearson, R. G. *J. Am. Chem. Soc.* **1963**, *85*, 3533.
(37) Cattalini, L.; Orio, A.; Nicolini, M. *J. Am. Chem. Soc.* **1966**, *88*, 5734-5738.
(38) Elding, L. I.; Olsson, L. F. *J. Phys. Chem.* **1978**, *82*, 69-74.

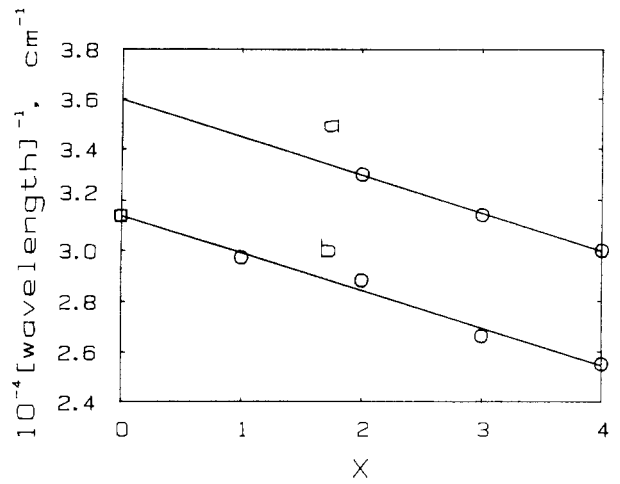

Figure 9. Linear relationships between $1/\lambda_{max}$ of Pt(II) complexes and number of chloride ions in the complex: (a) $d_{xz,yz} \rightarrow d_{x^2-y^2}$ transition (slope = $-(1.49 \pm 0.04) \times 10^{-4}$ nm^{-1}, intercept = $(3.60 \pm 0.02) \times 10^{-3}$ nm^{-1}); (b) $d_{xy} \rightarrow d_{x^2-y^2}$ transition (slope = $-(1.5 \pm 0.2) \times 10^{-4}$ nm^{-1}, intercept = $(3.13 \pm 0.05) \times 10^{-3}$ nm^{-1}).

larger ϵ values for this transition, while the ϵ values for the $d_{xy} \rightarrow d_{x^2-y^2}$ band change very little.

The law of average environment states that the crystal field Δ value for a mixed-ligand octahedral complex is given by the weighted average of the Δ values for each of the individual ligands.[39] We find that a similar relationship exists for the square-planar complexes. Plots of the reciprocals of λ_{max} of the $PtCl_x(OH)_{4-x}^{2-}$ complexes vs x (the number of chloride ions coordinated to Pt(II)) give straight lines (Figure 9) for both absorption bands. The plot of the $d_{xy} \rightarrow d_{x^2-y^2}$ transition has an intercept of 3.60×10^{-3} nm^{-1}, and that of the $d_{xz,yz} \rightarrow d_{x^2-y^2}$ transition, 3.13×10^{-3} nm^{-1}. The latter is seen as a shoulder at 320 nm in the resolved spectrum of $Pt(OH)_4^{2-}$. The correlation predicts another d-d transition for $Pt(OH)_4^{2-}$ at 278 nm, but the intense charge-transfer bands below 250 nm mask this absorption band.

(39) Sutton, D. *Electronic Spectra of Transition Metal Complexes*; McGraw-Hill: London, 1968; p 162.

Acknowledgment. This work was supported by Public Health Service Grant No. GM12152 from the National Institute of General Medical Sciences. We are grateful to Robert E. Santini for his assistance in the NMR experiments.

Appendix. Validity of Assignment of Reaction Times for the ^{195}Pt NMR Kinetic Data

For the ^{195}Pt NMR data used in the evaluation of the rate constants, the intensity of the signal, I_{exp}, was obtained from the integrated average over a 1-h period. The time assigned in this evaluation, t_{exp}, was the midpoint of the time interval. Since the actual time (t_{act}) when the intensity is equal to I_{exp} is not exactly at the midpoint, it is necessary to check the validity of using t_{exp} instead of t_{act}.

For a first-order reaction

$$I = I_0 e^{-kt} \tag{A1}$$

$$I_{exp} = 1/(t_2 - t_1) \int_{t_1}^{t_2} I \, dt = \frac{I_0}{k(t_2 - t_1)} (e^{-kt_1} - e^{-kt_2}) \tag{A2}$$

where t_1 and t_2 are the initial and final times used to obtain the signal.

When $t = t_{act}$

$$I_{exp} = I_{act} = I_0 e^{-kt_{act}} \tag{A3}$$

Equating eq A2 and eq A3 permits t_{act} to be evaluated:

$$t_{act} = -\frac{1}{k} \ln \left[\frac{e^{-kt_1} - e^{-kt_2}}{k(t_2 - t_1)} \right] \tag{A4}$$

When $t_1 = 1800$ s, $t_2 = 5400$ s, and $k = 7.2 \times 10^{-5}$ s^{-1}, eq A4 gives $t_{act} = 3561$ s. This is very close to the t_{exp} value used: $(t_1 + t_2)/2 = 3600$ s. Hence the experimental error in the time assignment is only 1% for the fastest rate and is less for other measurements.

Contribution from the Department of Physical and Inorganic Chemistry, University of Adelaide, Adelaide, South Australia 5001, Australia

Complexation of Lithium Ion by the Cryptand 4,7,13-Trioxa-1,10-diazabicyclo[8.5.5]eicosane (C21C$_5$) in a Range of Solvents. A ^{7}Li Nuclear Magnetic Resonance and Potentiometric Titration Study

Stephen F. Lincoln* and Amira Abou-Hamdan

Received October 25, 1989

Complexation of Li^+ by the cryptand 4,7,13-trioxa-1,10-diazabicyclo[8.5.5]eicosane (C21C$_5$) to form the cryptate $[Li.C21C_5]^+$ has been studied in eight solvents by ^{7}Li NMR and potentiometric titration methods. The variation of the ^{7}Li chemical shift of $[Li.C21C_5]^+$ with solvent and a comparison of its stability with those of other cryptates indicate that $[Li.C21C_5]^+$ exists substantially in the *exclusive* form in solution in contrast to the *inclusive* form adopted in the solid state. The exchange of Li^+ on $[Li.C21C_5]^+$ is within the ^{7}Li NMR time scale in methanol, dimethylformamide, diethylformamide, and dimethylacetamide, where, in the last solvent at 298.2 K, the logarithm of the $[Li.C21C_5]^+$ stability constant [log (K/dm^3 mol^{-1})] is 1.85 and the decomplexation kinetic parameters are $k_d = 237 \pm 4$ s^{-1}, $\Delta H_d^* = 49.0 \pm 2.1$ kJ mol^{-1}, and $\Delta S_d^* = -35.0 \pm 2.8$ J K^{-1} mol^{-1}. Similar data are obtained in the other three solvents. In acetonitrile, propylene carbonate, and acetone, Li^+ exchange is too slow to be studied by ^{7}Li NMR spectroscopy. The $[Li.C21C_5]^+$ data are compared with those for $[Li.C211]^+$, $[Na.C21C_5]^+$, and $[Na.C211]^+$.

Introduction

Studies of the complexes, or cryptates, formed between alkali-metal ions and poly(oxadiazabicycloalkane) ligands, or cryptands, have produced a substantial understanding of the effects of metal ion size and cryptand cavity size on the structure, stability, and lability of cryptates, and the mechanisms of cryptate complexation processes.[1-16] Recently attention has turned to the effect of the cryptand donor atoms on these characteristics of the com-

(1) Lehn, J.-M. *Struct. Bonding (Berlin)* **1973**, *16*, 1-69.
(2) Lehn, J.-M. *Acc. Chem. Res.* **1978**, *11*, 49-57.
(3) Lehn, J.-M. *J. Inclusion Phenom.* **1988**, *6*, 351-396.

0020-1669/90/1329-3584$02.50/0